Local similarity measures for lesion registration in DCE-MRI of the breast

Sebastian Schäfer[a]*, Uta Preim[b], Sylvia Glaßer[a], Bernhard Preim[a] and Klaus Tönnies[a]

[a] Department of Simulation and Graphics,
University of Magdeburg, Germany

[b] Herzzentrum Leipzig,
University of Leipzig, Germany

* Corresponding author's email address: ⟨sebastian.schaefer@ovgu.de⟩

Abstract

Dynamic contrast-enhanced MRI (DCE-MRI) of the breast is widely used for detection and quantification of breast cancer. Patient motion influences the correct determination of perfusion characteristics, an important indicator for diagnostic purposes. This work presents an evaluation of three similarity measures for local region of interest registration of lesions in DCE-MRI. We evaluate rigid and non-rigid registration results using a pharmacokinetic model and compare measured perfusion data to the modelled function values. In addition, acquisitions from different time frames are used (pre- and post-contrast) as fixed image and a masked calculation of similarity to observe the influence on the registration quality. The best results are achieved with non-rigid transformation and a post-contrast fixed image leading to an average improvement between 3.9 % and 16.8 % in terms of the fitting quality to the pharmacokinetic model.

1   Introduction

Breast cancer is the most common form of cancer and the most common cause of cancer-related death in women in 2008 [Boyle and Levin, 2008]. Progress in early detection, diagnosis and treatment planning of invasive breast lesions is an important part to improve cure [Schreer and Lüttges, 2005]. Dynamic contrast-enhanced MRI (DCE-MRI) of the breast is known to be a very sensitive modality for invasive breast cancer and the detection of small lesions. However, specificity is moderate compared to conventional X-ray mammography [Kuhl, 2007]. This is why DCE-MRI is also used as complementary method to reveal small tumours in the surroundings of a primarily detected tumour. Additionally, it is able to gain information about perfusion kinetics which describe the changes in contrast over time in various parts of a lesion. It is also preferred with younger patients because the dense tissue

of the breast attenuates the signal of standard X-ray mammography. This is particular relevant in high-risk cases, where relatives of the patient (sister or mother) suffered from breast cancer early. Furthermore, there is great interest to improve the separability of benign and malignant cancer lesions by the help of perfusion enhancement characteristics.

Perfusion imaging like DCE-MRI is used to display blood distribution within the human body by acquiring multiple 3D volumes (also referred to as 4D imaging). The blood flow of specific body parts is visualised through an injected contrast agent (CA) of gadopentetic acid (Gd-DTPA) [Heywang et al., 1986]. The signal change over time can be observed and reveals perfusion. DCE-MRI for breast cancer diagnosis highlights suspicious tumours inside the female breast, because malignant tumours lead to formation of new vessels (angiogenesis) which accumulate contrast-enhanced blood.

In dynamic imaging, identical conditions cannot be guaranteed to be achieved for each instance of a time series. Apart from camera system-dependent influences like noise artefacts, patient motion poses a main problem. This motion evokes false inter-voxel correspondences between different time acquisitions [Guo et al., 2006]. It leads to incorrect assumptions in diagnosis and thus hampers correct classification of tumours. As DCE-MRI is very sensitive to detect small enhancing structures [Kuhl, 2007], motion influence has a particularly strong impact on those small tumours. Investigations in this work are concentrated on lesions which are smaller than 10 mm in at least one dimension.

To compensate for motion influence, registration algorithms try to find a transformation to align images by optimising a similarity measure indicating best matchings between time step images. In general, registration approaches aim at finding the best solution minimising a global criterion on the whole image. If a region of interest (ROI) – representing a part of the whole dataset – is examined, it cannot be assumed that the best possible matching in terms of the local observation is obtained from a global matching. This is why we need a local area registration.

We employ rigid and non-rigid transformations for the registration procedure to process ROI of breast lesions taking into account the local similarity. Therefore, we investigate the performance of three different standard criteria Mutual Information (MI), Mean Squared Distance (MSD) and Normalized Correlation (NC) to analyse how they cope with the particular scenario of varying intensities. Through the use of a manually generated binary mask defining perfused and non-perfused areas, the similarity can optionally be limited to be calculated with non-perfused parts.

Finally, the evaluation of differently parametrised experiments to assess the performance of the local similarity criteria is measured by the use of a pharmacokinetic model [Radjenovic et al., 2008] which simulates the concentration of CA at specific time points after the injection. The measured MRI signal enhancement in pathological tissue before and after the registration is compared to the simulated signal in order to obtain a fitting error. This evaluation is based on the assumption that a better fit of the model parameters indicates a better motion correction. We chose this indirect method since no ground truth is available. 50 lesions from 45 different patients have been assessed in this investigation. The clinical research goal of that data collection was to assess heterogeneity of breast tumours as an indicator for malignancy [Preim et al., 2011, to appear].

2   Related Work

A non-rigid registration procedure is required for DCE-MRI data of the breast, because the soft tissue leads to deformation that cannot be described by affine transformations. Guo et al. [2006] give a survey about recent approaches of breast image registration techniques, including DCE-MRI. The more advanced techniques use a global to local strategy by applying affine transformation and non-rigid transformation sequentially [Rueckert et al., 1999, Rohlfing et al., 2003] or simultaneously [Fischer and Modersitzki, 2002]. This does not produce optimal results for ROI with small enhancing lesions for two reasons. First, areas with constant intensity values have a stronger influence on the transformation. Consequently the areas of tumorous tissue with changing intensity over time yield less stronger similarity measures resulting in less influence on the transformation. Second, the local transformations result in a compromise that is optimal for the whole image. In contrast, we search for a registration and a best fit for a ROI representing a tumour lesion only.

Tofts et al. [1995], Hoffmann et al. [1995] have published the first pharmacokinetic models to quantitatively analyse DCE-MRI data of the breast. Thus, they link the physics of the MRI signal acquisition and the underlying physiology that governs CA kinetics. The CA concentration is calculated depending on physical properties, acquisition-related parameters and the physiological character of tissue. In general, the latter is unknown and thus is determined by fitting the function to the concentration measured in the image data, leaving physiological values as free parameters. Radjenovic et al. [2006] adapted the model function from Brix et al. [1991] and Tofts et al. [1995]. A practical clinical study was performed by Radjenovic et al. [2008] to show the applicability for differently graded invasive human breast tumours. The model was able to adapt to all measured curves in the study. Statistically significant variation was only measured along two permeability-related physiological parameters. We use it to evaluate our registration results by measuring the distance between observed values and model generated values which are only determined by the two physiological parameters.

Hayton [1998] proposes a framework for registration of DCE-MRI which uses the pharmacokinetic model of Tofts et al. [1995] to explain the change of intensity. Transformation parameters for registration are derived from minimization of the mean squared error between measured time signal and modelled curve.

For the analysis of DCE-MRI of the breast we propose a region segmentation of breast lesions to combine similar perfusion characteristics and lower the influence of noise compared to a single voxel-based consideration [Glaßer et al., 2009]. This approach also provides a detailed and comprehensive diagnostic utility.

We use a combination of the segmentation approach of Glaßer et al. [2009] and a fitting of the perfusion characteristics to the pharmacokinetic model described in [Radjenovic et al., 2008] to test different registration parametrisations.

First results of a model-based evaluation have been presented in [Schäfer et al., 2010]. The study comprised 20 lesions and used rigid transformations for registration. In contrast, the study in this work includes more samples containing also ROI larger than 10 mm in one dimension. Therefore, we incorporate non-rigid transformations to compensate for non-linear types of deformation.

3   Registration

The registration is performed on defined ROI assuming one volume out of the series to be fixed and finding transformations for each of the remaining volumes to match the fixed image. For each suspicious lesion one cuboid ROI is defined such that it fully includes the enhancing tissue to be examined in all time steps. The definition of the ROI is carried out by our medical collaborator, a radiologist specialized in the diagnosis of breast cancer. At the same time, a binary mask is created to define voxels being part of tumorous tissue for later use in a masked registration. This mask is generated by applying an enhancement threshold value between 50% and 100% between any of the contrast images and the pre-contrast image. The masks have been edited and corrected by our collaborator slice-wise to include parts of the tumour with weak contrast agent enhancement, e.g. necrotic tissue.

We want to investigate the performance of different similarity measures to determine the capability to compensate for motion in the presence of noise and signal variation due to CA enhancement in the ROI. We choose the commonly used criteria MI (as described by Mattes et al. [2003], Eq. 1), MSD (Eq. 2) and NC (Eq. 3).

$$MI(\lambda, \kappa, \mu) = -\sum_{\lambda} \sum_{\kappa} p(\lambda, \kappa | \mu) log \frac{p(\lambda, \kappa | \mu)}{p_M(\lambda, \mu) p_R(\kappa)} \tag{1}$$

$$MSD(A, B) = \frac{1}{N} \sum_{i=1}^{N} \left(A_i - B_i)^2 \right) \tag{2}$$

$$NC(A, B) = \frac{\sum_{i=1}^{N} \left(A_i \cdot B_i \right)}{\sqrt{\sum_{i=1}^{N} A_i^2 \cdot \sum_{i=1}^{N} B_i^2}} \tag{3}$$

λ and κ are indices of uniformly sized histogram bins, μ is the vector holding transformation-specific parameters, and p, p_M, p_R are the joint, marginal moving image and marginal fixed image probability distributions, respectively. A_i and B_i are the ith voxels of an image A and B, respectively. N is the total number of voxels.

We aim to register a set of dynamic images that focus on regions showing perfusion dynamics. MI is used to register images acquired with different modalities as it takes the joint entropy of two images into account. In DCE-MRI data, the images are from the same modality, but are showing different image intensity levels. The MSD measure aligns voxels showing same intensities, which cannot be generally assumed in our case. However, there are parts of the images showing no dynamics and thus fulfilling the requirement. We expect these parts – the surroundings of enhancing structures – to be sufficiently dominating to guide the registration process. The NC metric calculates statistical correlation between configurations of intensities and compensates for multiplicative intensity factors through normalization.

Registration of the lesion depicting ROI (Fig. 1 (a)) is performed using rigid transformations, non-rigid B-Spline-based transformations and both subsequently (Fig. 1 (d)) for each of the local similarity measures MI, MSD and NC. Additionally, each investigation is registered to the pre-contrast time step volume and to the second post-contrast time step volume. In the pre-contrast phase enhancing structures are not visible and cannot be used in registration. Similarity between different time step volumes is increased using a post-contrast volume as fixed image. The influence of using both as fixed volume is investigated. We use the second post-contrast time step ($t = 2$) because we can expect the contrast agent to be
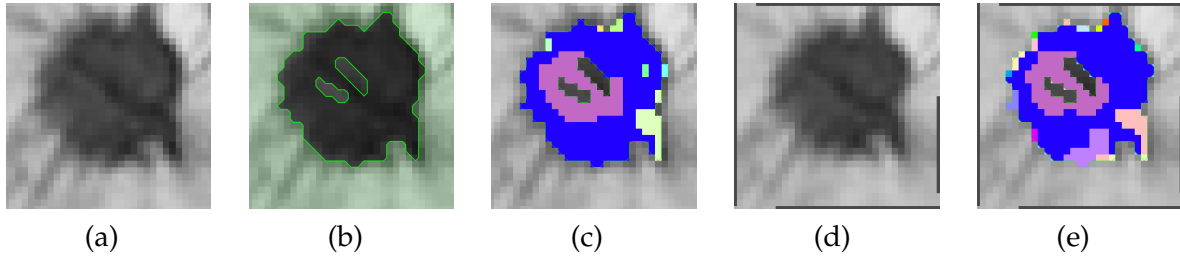
    (a)   (b)   (c)   (d)   (e)

Figure 1: (a) Slice of a dataset volume at time $t = 0$. (b) The same slice depicted with the binary mask. (c) Regions generated by the segmentation approach before registration. (d) Slice of the dataset volume at time $t = 0$ after consecutive rigid and B-Spline-based registration. (e) Regions generated by the segmentation approach after registration.

diffused in the whole tumour for healthy and pathologic tissue. Furthermore, for each investigation, we use manually created binary segmentations (Fig. 1 (b)) which define a voxel as perfused or non-perfused to exclude perfused areas of the dataset for the calculation of local similarity. The hypothesis is that a higher accordance of the similarity measures in unperfused areas supports the registration quality, especially in case of MSD, which handles intensity variations as the least of all measures. For evaluation purposes, the lesion is segmented using the region merging procedure of Glaßer et al. [2009]. Fig. 1 (c) and (e) show the differences of segmentation results before and after segmentation meaning that the perfusion characteristics have been altered by registration.

All registrations are performed using the ITK software toolkit [Ibanez et al., 2005]. Transformation parameters have been optimized using the bounded limited-memory Broyden-Fletcher-Goldfarb-Shanno algorithm (LBFGSB). Rigid transformations are bounded to 2 mm maximum translation and a rotation angle of $\pm 20°$. B-Spline grid points are allowed to move half the distance of the point spacing. A system with 8×8 grid points is used including stabilizing Spline points outside the image.

4   Evaluation

There is no ground truth data available for evaluation because the true motion shift and deformation of tissue are unknown. We decided to use the properties of the perfusion and the CA distribution to measure the accuracy of different registration configurations. Therefore, the pharmacokinetic model function described in [Radjenovic et al., 2008] is employed to produce CA concentration over time from the manually masked areas where perfusion is present. The signal intensity SI can be calculated at time t with the two free physiologic parameters v_e and k_{ep} defining the leakage space and capillary permeability using Eq. 7.

The approach uses acquisition-related parameters (D, T, $T1$ and τ) and physical constants (k_{el}^W, a_1, a_2) taken from Radjenovic et al. [2008] as well as the camera-related parameter TR. SI_0 is the pre-injection signal at $t = 0$ and $R1 = 4,5 \ mMols^{-1}$ is a relaxivity constant[1].

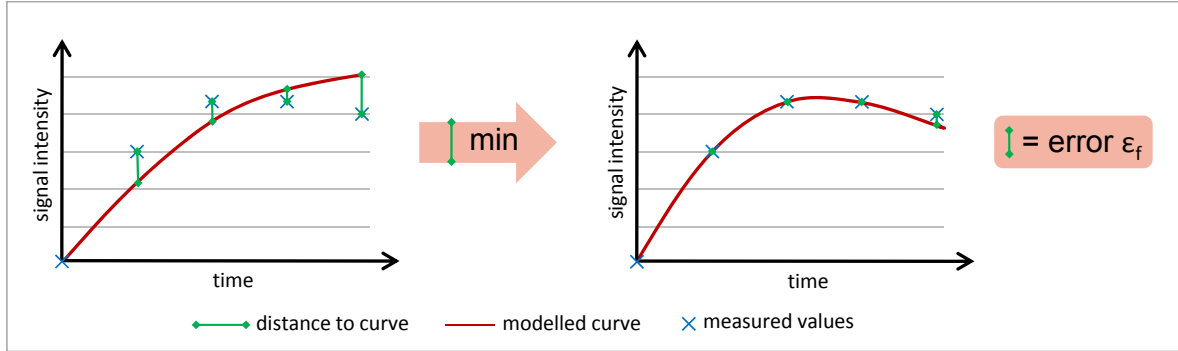[1]see [Radjenovic et al., 2008] for more details on parameters

Figure 2: Schematic description of the model fitting process and determination of the remaining fitting error ϵ_f.

$$v = \frac{1}{k_{ep} - k_{el}^W} \tag{4}$$

$$u = \frac{k_{ep}v}{k_{el}^W} \tag{5}$$

$$C_t(t, v_e, k_{ep}) = v_e \frac{D(a_1 + a_2)}{T} \left(u \left(e^{k_{el}^W \tau} - 1 \right) e^{-k_{el}^W t} - v \left(e^{k_{ep}\tau} - 1 \right) e^{-k_{ep}t} \right) \tag{6}$$

$$SI(t, v_e, k_{ep}) = \left(1 + \left(\left(\frac{e^{\frac{-TR}{T1}}}{1 - e^{-\frac{-TR}{T1}}} \right) TR \cdot R1 \right) C_t(t, v_e, k_{ep}) \right) SI_0 \tag{7}$$

By varying the two physiologic parameters v_e and k_{ep} and fitting the resulting function values of $SI(t)$ to the signal enhancement of measured data (Fig. 2) through regression analysis, the lowest mean absolute difference error ϵ_f is determined:

$$\epsilon_f = \sum_{t=0}^{n} |SI(t, v_e, k_{ep}) - M(t)| \to \min_{v_e, k_{ep}}. \tag{8}$$

36 differently parametrized procedures are performed to assess each combination of parameters for registration, which are:

- three different transformation types: rigid (translation and rotation), non-rigid (B-Spline-based), both combined sequentially,

- two different fixed volumes: pre-contrast ($t = 0$) and a post-contrast volume (e.g. $t = 2$),

- masked and unmasked calculation of local similarity,

- three different similarity measures: MI, MSD and NC.

Before and after performing registration, the dataset is evaluated by the pharmacokinetic model analysis. Therefore, a lesion is segmented (Fig. 1 (c) and (e), Fig. 3 (f)). Neighbour regions are merged if the averaged perfusion time curves of both current regions exceed a
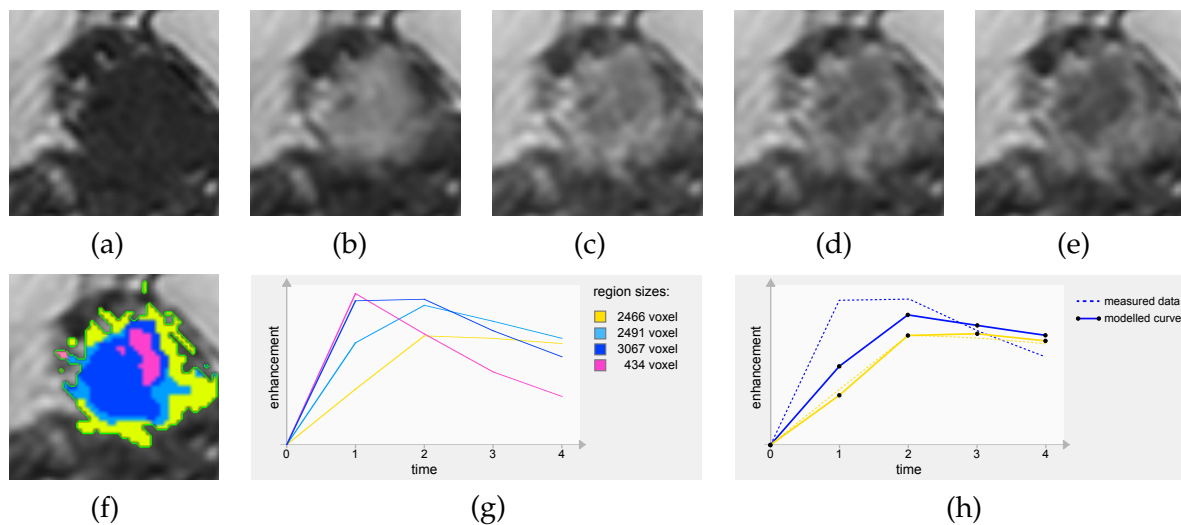
Figure 3: Images from (a) to (e) show enhancing tissue over time in one slice of the 3D volume. (f) depicts regions generated by the region merging procedure each with a different perfusion curve (g). For two of the regional perfusion curves (blue and yellow, dotted) the modelled perfusion curves with minimal distance (solid) to the measured values are shown in (h).

correlation of 95 % (Pearson's correlation coefficient is used). This has proven to be a suitable value to distinguish between homogeneous lesions yielding only one bigger region and heterogeneous lesions yielding multiple regions of about the same size. Using correlation to compare the curve signals merges regions with similar curve characteristics although the absolute intensity values could vary. After the region merging procedure, pharmacokinetic model evaluation is applied to the averaged regional time curves. This reduces the influence of noise compared to single voxel analysis and the number of curve fitting processes. The weighted average of resulting minimal fitting errors ϵ_f for all regions containing at least 6 voxels are computed according to the size of the region. We omit the calculation of fitting errors for small regions as they are of no diagnostic relevance. For each registration experiment the change of the average error is observed in comparison with the error measured before registration.

Figure 3 (f, g) shows an example of the region merging result and the regional perfusion curves. Additionally, the modelled curves are shown (Fig. 3 (h)). For the yellow region the resulting fitting error will be very small, because the model parameters could be adjusted, such that measured values and simulated perfusion are fitting accurately. In contrast, the model was not able to produce a curve to fit the blue regional perfusion curve well. This will result in a higher fitting error for this region.

5 Results and Discussion

We carried out the described procedure for 50 lesions from 45 different patient datasets. The datasets have been acquired with a 1.5 T MRI scanner (Philips Medical Systems) using a Spoiled Gradient Echo Sequence with TR ≈ 11 ms, TE ≈ 6 ms and a flip angle of 25°.

For each patient 5–6 dynamic scans have been performed with varying temporal interval between 62 s and 110 s. The first scan is performed without CA, thus it is often referred to as pre-contrast image (Fig. 3 (a)). At the end of the first scan, CA is injected and can be observed from the second time step image on. Therefore, these images are denoted as post-contrast images (Fig. 3 (b-e)). The spacing between voxels is ≈ 0.6 mm, the slice spacing is 1.5 mm. Results are presented with respect to the used fixed volume image, the transformation types, the influence of the binary mask and the similarity measures. Changes of the fitting error $\Delta\epsilon$ with the pharmacokinetic model before (ϵ_{pre}) and after (ϵ_{post}) registration are expressed as a percentage of improvement $\Delta\epsilon = \frac{\epsilon_{pre}}{\epsilon_{post}} - 1$.

Fixed image volume: As expected, the post-contrast volume used as fixed image for registration generally leads to higher fitting quality (averaged over all other parameters: 8.4 % improvement of the fitting quality compared to 2.9 %). This is accounted for by the structural differences between pre- and post-contrast volumes. Enhancing structures are not yet visible in pre-contrast volumes which makes registration difficult. Using a post-contrast volume image as registration basis improves registration at least for the remaining post-contrast images, if not necessarily for the pre-contrast image. Nevertheless, registration of all post-contrast volumes to the first time volume is not advisable and will not be included in the further discussion.

Transformations: Comparing the charts in Figure 4 (a) and (c), non-rigid transformation produces better results in terms of the pharmacokinetic model evaluation compared to rigid transformation (10.8 % compared to 3.8 %). The ROI are affected by non-linear deformation which is better corrected for by the B-Spline-based transformation. The results of the combined rigid and non-rigid transformations (Fig. 4 (e)) do not differ significantly from the B-Spline-based results (averaged 10.6 % compared to 10.9 %). This is due to the fact that the slight translation and rotation shifts (not more than 2 mm and 20°) in the ROI can be compensated by B-Spline transformation. Using rigid registration, 34.0 % of the datasets yield a decreased fitting quality (Fig. 4 (b)), whereas for registration including non-rigid transformation only 17.2 % of the datasets lead to decreased fitting quality (Fig. 4 (d, f)).

Masked registration: In general, masking the calculation of the similarity does not result in improved fitting quality (8,7 % for unmasked calculation compared to 8,1 % for masked calculation). For rigid registration the masked similarity calculation leads to a higher fitting error for all three similarity measures. The masked calculation results in a reduction of possible locations to calculate similarity from, as translations of up to 3 voxels are applied, shifting the boundary of the lesions out of overlap. However, in case of MSD and non-rigid based transformations, the calculation of similarity with masked similarity calculation has a positive influence on the evaluation of the fitting error (4.3 % improvement without mask compared to 7.6 % with mask). Hence, when using MSD, a masked registration is appropriate to reduce the fact that MSD is not capable to handle the variation in intensity. For MI and NC combined with non-rigid transformations no improvement has been observed (13.2 % for unmasked compared to 13.1 % for masked calculation). Both similarity measures are able to deal with the different intensity levels due to contrast enhancement.
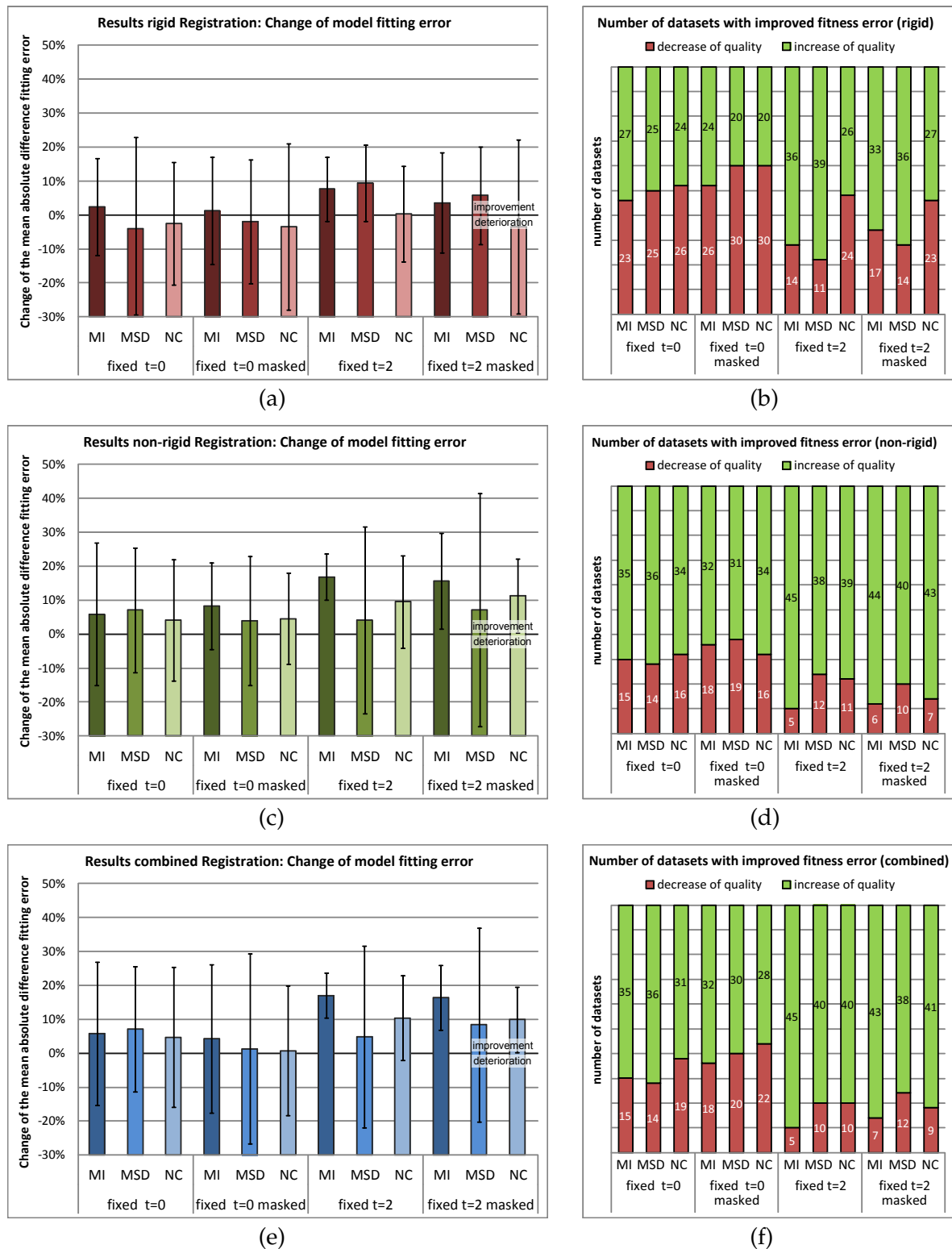
Figure 4: Registration Results: Average change and standard deviation of the model fitting error and the number of samples with improved model fitness error: rigid transformation (a, b), non-rigid transformations (c, d) and both registrations combined (e, f).
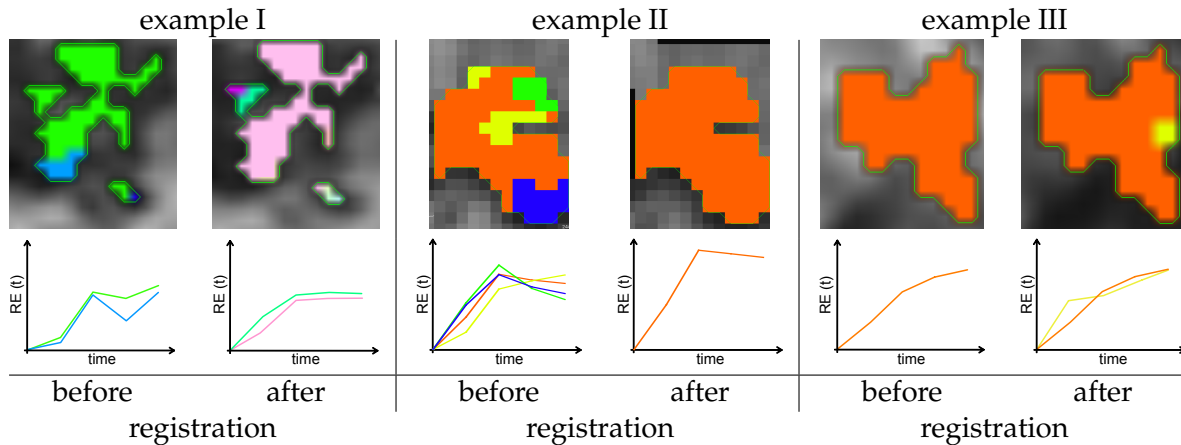
Figure 5: Perfusion time curves showing relative enhancement (RE) of regions in a representative slice before and after the registration procedure for three different datasets. Registration has been performed with non-rigid transformation and MI as similarity measure in each of the cases.

Similarity measures: Overall, MI provides the best improvement rate in terms of the fitting error considering the $t = 2$ volume as fixed image (12.7 % averaged over transformation types and masked/unmasked registration). For non-rigid registration it also exhibits the smallest amount of lesions with a decreased fitting quality compared to the error before registration, 10 % and 12 % of the lesions for unmasked and masked registration, respectively (Fig. 4 (d)). MI also yields the best result within the study with 16.8 % of error improvement for combined transformation with post-contrast fixed image and unmasked calculation used as fixed image. The standard deviation of the fitting error is smaller especially compared to MSD but also compared to NC.

In general, results generated with MSD-based similarity calculation have similar performance compared to NC (6.5 % and 6.3 %). However, the number of datasets with a decreased fitting quality was 23.0 % for MSD and 28.0 % for NC measure, overall. MSD yields the best results compared to the other similarity measures when rigid transformation is used (7.6 % for MSD compared to 5.6 % for MI and -1.5 % for NC). NC outperforms MSD in combination with non-rigid transformations (10.1 % compared to 6.0 %). It also produces less datasets with increased fitting error with non-rigid transformations being used (18 % for non-rigid based transformations compared to 46 % for rigid transformation).

NC is the most sensitive measure towards the parametrisation in this study ranging between -3.4 % and 11.1 %. In comparison to Schäfer et al. [2010] it is not able reach as good results as the other two similarity criteria. As a major difference, this study includes more ROI depicting bigger lesions. This seems to have not only an influence on the transformation, but also on the NC measure, because the proportion of perfusion enhanced and non-perfusion enhanced voxels differs with the size of the ROI or lesion.

Figure 5 illustrates three examples (a representative slice of the volume is shown) with perfusion regions and associated perfusion time curves before and after the registration procedure. The curve plots only depict regions of at least 6 voxels. Example (I) shows visually improved perfusion behaviour after registration. The time course of both regions is smoother and more plausible according to physiologic behaviour. Example II exhibits mul-

tiple regions before registration, where perfusion characteristics are mixed due to motion. After registration the segmentation approach only finds a single region representing the tumour. The resulting time signal curve has a lower fitting error to the pharmacokinetic model. Example III is a dataset where the overall fitting quality has decreased due to an introduced region (yellow) after registration at the border which does not coincide well with the pharmacokinetic model assumptions.

6   Conclusions

We compared three different similarity measures for ROI-based registration of contrast-enhancing lesions in DCE-MRI data of the breast. Additionally, the impact of different transformation functions, rigid and non-rigid, the used fixed image and a mask eliminating perfused parts from similarity calculation have been tested using a pharmacokinetic model evaluation.

Improvements have been achieved by using all similarity measures, if a post-contrast volume is used as fixed image for registration (Fig. 4). Using pre-contrast volumes as fixed image hampers the calculation of similarity. This is due to the fact that some enhancing structures are simply not yet visible in pre-contrast volumes. If rigid transformation is used, the evaluation measure deteriorates. For non-rigid transformations the improvements lag behind the post-contrast fixed volume registrations. Thus, the post-contrast volume $t = 2$ as fixed image is considered as applicable.

Overall, best results are achieved using non-rigid transformation. The combined registration (rigid and subsequent B-Spline transformation) produces similar results for all other parameters, whereas rigid registration alone is not able to keep up with the other two methods. MI performs best for non-rigid transformations with 16.0 % and 16.5 % improvement of the fitting error for B-Spline solely and combined rigid B-Spline, respectively. Using MSD as similarity measure achieves best fitting error values for rigid registration with 7.5 % for post-contrast fixed volume registration. NC yields only moderate results, especially with rigid transformation used, it is not able to improve the fitting error to the physiological model when masked similarity calculation is used. MI is able to produce slightly better results when enhancing tissue is not masked out in similarity calculation. However, using MSD measure, results could be improved when enhancing parts of the lesion are left out (for non-rigid based transformations).

The evaluation using a pharmacokinetic model shows that the fit in relation to measured data improves through local registration. This improves the image information relevant for breast tumour diagnosis. A consequent step would be to use the model fitting error as optimisation criterion for registration. However, two aspects should be considered. First, perfusion characteristics are not at all homogeneous within a lesion [Glaßer et al., 2009] and registration towards an ideal model concept might blur the boundaries of perfusion areas. Second, slight changes in the model description parameters v_e and k_{ep} may result in better fitting errors in terms of the model, but may alter the diagnostic meaning of the perfusion time curve. Hence, in our opinion, an optimisation of transformation parameters should be controlled by both, local similarity based on intensity (primarily of the surrounding area) and the fitting quality with a pharmacokinetic model description of the time curves.

This study also indicates that motion influence in DCE-MRI data of the breast has an impact on the analysis of perfusion characteristics. Future work will be targeted on the

consequences of motion correction by registration on diagnosis of small enhancing lesions in this data.

7 Acknowledgement

References

P. Boyle and B. Levin. World cancer report 2008. *Int. Agency for Research on Cancer*, 2008.

G. Brix, W. Semmler, R. Port, L.R. Schad, G. Layer, and W.J. Lorenz. Pharmacokinetic parameters in CNS Gd-DTPA enhanced MR imaging. *Journal of Computer Assisted Tomography*, 15 (4):621–8, 1991.

B. Fischer and J. Modersitzki. Curvature based registration with applications to MR-mammography. In *Int. Conference on Computational Science (ICCS)*, pages 202–206, 2002.

S. Glaßer, S. Schäfer, S. Oeltze, U. Preim, K.D. Tönnies, and B. Preim. A visual analytics approach to diagnosis of breast DCE-MRI data. In *Vision Modelling and Visualzation*, pages 351–362, 2009.

Y. Guo, R. Sivaramakrishna, C.C. Lu, J.S. Suri, and S. Laxminarayan. Breast image registration techniques: a survey. *Medical and Biological Engineering and Computing*, 44(1):15–26, 2006.

P.M. Hayton. *Analysis of contrast-enhanced breast MRI*. PhD thesis, University of Oxford, October 1998.

S.H. Heywang, D. Hahn, H. Schmidt, I. Krischke, W. Eiermann, R. Bassermann, and J. Lissner. MR imaging of the breast using gadolinium-DTPA. *Journal of Computer Assisted Tomography*, 10(2):199, 1986.

U. Hoffmann, G. Brix, M. V. Knopp, T. Heß, and W.J. Lorenz. Pharmacokinetic mapping of the breast: a new method for dynamic MR mammography. *Magnetic Resonance in Medicine*, 33(4):506–514, 1995.

L. Ibanez, W. Schroeder, L. Ng, and J. Cates. *The ITK Software Guide*. Kitware Inc., second edition, 2005.

C.K. Kuhl. The current status of breast MR imaging, part I. *Radiology*, 244(2):356–378, 2007.

D. Mattes, D.R. Haynor, H. Vesselle, T.K. Lewellen, and W. Eubank. PET-CT image registration in the chest using free-form deformations. *IEEE Trans. Medical Imaging*, 22(1):120–128, 2003.

U. Preim, S. Glaßer, B. Preim, F. Fischbach, and J. Ricke. Computer-aided diagnosis in breast DCE-MRI-quantification of the heterogeneity of breast lesions. *European Journal of Radiology*, 2011, to appear.

A. Radjenovic, J.P. Ridgway, and M.A. Smith. A method for pharmacokinetic modelling of dynamic contrast enhanced mri studies of rapidly enhancing lesions acquired in a clinical setting. *Physics in Medicine and Biology*, 51:N187–97, 2006.

A. Radjenovic, B.J. Dall, J.P. Ridgway, and M.A. Smith. Measurement of pharmacokinetic parameters in histologically graded invasive breast tumours using dynamic contrast-enhanced MRI. *British Journal of Radiology*, 81(962):120–128, 2008.

T. Rohlfing, C. R Maurer, D. A Bluemke, and M. A Jacobs. Volume-preserving nonrigid registration of MR breast images using free-form deformation with an incompressibility constraint. *IEEE Trans. Medical Imaging*, 22(6):730–741, 2003.

D. Rueckert, L.I. Sonoda, C. Hayes, D.L.G. Hill, M.O. Leach, and D.J. Hawkes. Nonrigid registration using free-form deformations: application to breast MR images. *IEEE Trans. Medical Imaging*, 18(8):712–721, 1999.

S. Schäfer, C.M. Hentschke, and K.D. Tönnies. Local similarity measures for roi-based registration of DCE-MRI of the breast. In *Proc. Medical Image Understanding and Analysis (MIUA)*, pages 159–163, 2010.

I. Schreer and J. Lüttges. Breast cancer: early detection. *Radiologic-Pathologic Correlations from Head to Toe*, pages 767–784, 2005.

P. S. Tofts, B. Berkowitz, and M.D. Schnall. Quantitative analysis of dynamic Gd-DTPA enhancement in breast tumors using a permeability model. *Magnetic Resonance in Medicine*, 33(4):564–568, 1995.